

# Structural and electrochemical analysis of layered compounds from $\text{Li}_2\text{MnO}_3$

C.S. Johnson<sup>a,\*</sup>, S.D. Korte<sup>a</sup>, J.T. Vaughey<sup>a</sup>, M.M. Thackeray<sup>a</sup>, T.E. Bofinger<sup>b</sup>,  
Y. Shao-Horn<sup>b</sup>, S.A. Hackney<sup>b</sup>

<sup>a</sup> *Electrochemical Technology Program, Chemical Technology Division, Argonne National Laboratory, Argonne, IL, USA*

<sup>b</sup> *Department of Metallurgical and Materials Engineering, Michigan Technological University, Houghton, MI, USA*

## Abstract

Layered lithium-manganese-oxide electrodes with the general formula  $\text{Li}_{2-x}\text{MnO}_{3-x/2}$  ( $0 < x < 2$ ), and structural analogs in which some of the manganese has been substituted by Zr or Al have been prepared and characterized by structural and electrochemical methods. Although the discharge capacity for electrode compositions that contained Zr or Al fades at a slower rate in lithium cells than an unsubstituted compound,  $\text{Li}_{0.106}\text{MnO}_{2.053}$  ( $\text{Li}_{2-x}\text{MnO}_{3-x/2}$ , where  $x = 1.894$ ), these materials deliver lower capacities ( $\sim 90$  mA h/g after 20 cycles) than  $\text{Li}_{2-x}\text{MnO}_{3-x/2}$  when cycled between 3.8 and 2.0 V at a C/8–C/10 rate. Under humid conditions or in contact with carbon,  $\text{Li}_{2-x}\text{MnO}_{3-x/2}$  compounds transform slowly to  $\gamma\text{-MnO}_2$  on standing at room temperature, whereas the Zr- and Al-substituted materials appear to be more resistant to the conversion to  $\gamma\text{-MnO}_2$ . © 1999 Elsevier Science S.A. All rights reserved.

**Keywords:** Lithium battery; Lithium manganese oxide; Layered structure

## 1. Introduction

There has been considerable interest in the synthesis and the structural and electrochemical characterization of layered  $\text{LiMnO}_2$  compounds for lithium battery applications. In the past, most of the efforts to synthesize layered lithium-manganese oxides have focused on birnessite-type compounds that usually contain an appreciable amount of water within the layers [1–10]. Recently an anhydrous layered  $\text{LiMnO}_2$  material, which is isostructural with  $\text{LiCoO}_2$ , has been produced by ion-exchange of  $\alpha\text{-NaMnO}_2$  at the laboratories of Armstrong and Bruce [11] and Capitaine et al. [12]. Electrochemical and electron diffraction data indicate that the compound converts to a spinel-type structure on cycling with an unacceptable capacity fade [13,14].

Layered lithium manganese oxides have also been prepared by acid-leaching  $\text{Li}_2\text{O}$  from the rock-salt phase  $\text{Li}_2\text{MnO}_3$ . This reaction yields compounds with the general formula  $\text{Li}_{2-x}\text{MnO}_{3-x/2}$  ( $0 < x < 2$ ) [15]. The value of  $x$  is dependent on the acid concentration and leach time used for the reaction. We have continued this investigation

by varying the processing conditions to study the electrochemical behavior and structural stability of several substituted products. The ultimate objective of our work is to synthesize a stabilized layered lithium manganese oxide that does not convert to spinel. We selected  $\text{Li}_2\text{MnO}_3$  because it is easier to prepare than layered  $\text{LiMnO}_2$  and because it is possible to substitute some of the manganese ions in the structure with metal ions that form strong M–O bonds, for instance,  $\text{Zr}^{4+}$  or  $\text{Al}^{3+}$  ions.

## 2. Experimental

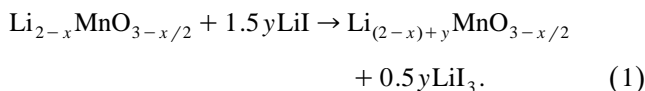
Standard  $\text{Li}_2\text{MnO}_3$  for the synthesis of  $\text{Li}_{2-x}\text{MnO}_{3-x/2}$  control samples was prepared by a conventional solid state reaction of stoichiometric amounts of  $\text{Li}_2\text{CO}_3$  and  $\text{MnCO}_3$  at 500°C for 72 h in air [15]. This material is designated ss/500C. The  $\text{Li}_{2-x}\text{MnO}_{3-x/2}$  ( $0 < x < 2$ ) materials were produced by acid-leaching  $\text{Li}_2\text{O}$  from the rock salt phase  $\text{Li}_2\text{MnO}_3$ . Substituted  $\text{Li}_2\text{MnO}_3$  samples were synthesized by the Pechini method [16]. A water solution (total end volume: 90–100 ml) consisting of an ethylene glycol/citric acid (0.075 mol/0.05 mol) mixture with lithium nitrate and manganese nitrate (52% in water) with a water soluble metal ion dopant (nitrate for Al, and oxynitrate for Zr) was

\* Corresponding author: Tel.: +1-630-252-4787; Fax: +1-630-252-4176; E-mail: johnsoncs@cmt.anl.gov

stirred and heated, first at 105°C to remove water, then slowly up to 300–400°C for gelling, drying and eventual combustion. The metal ion dopant was introduced into the mix at a nominal value of 5 mol%. (caution: this procedure can result in a highly exothermic reaction, producing hot NO<sub>x</sub> gases, and fire if the mixture is heated to dryness). The powders were subsequently calcined in air at 400°C for 2 h, followed by sintering at 700°C for 4 h. Materials made by this method are designated pch-M/700C. Zr<sup>4+</sup> can be substituted directly for Mn<sup>4+</sup>, whereas Al<sup>3+</sup> substitution requires additional Li<sup>+</sup> and less Mn<sup>4+</sup> to compensate for charge balance and stoichiometry.

In the acid-leaching step, sulfuric acid concentrations of 0.5 to 5.0 M were used. Mixing times ranged from less than 1 h to about 64 h. Samples were isolated by vacuum filtration, washed with water, and finally dried at 125°C for 16–24 h.

Acid-leached Li<sub>2</sub>MnO<sub>3</sub> products were lithiated chemically with LiI in acetonitrile at 80°C under N<sub>2</sub> according to the reaction [17]:



Lithiated materials were washed with acetonitrile and dried overnight at room temperature under vacuum. The chemical reversibility of reaction (1) was investigated by reacting the lithiated product with a 10% molar excess of bromine ( $E^\circ = 4.1$  V vs. Li) dissolved in chloroform. The reaction was carried out under nitrogen at room temperature. For simplicity, with  $x = 2$  and  $y = 1$ , this reaction can be represented as follows:



The concentrations of manganese and lithium in the various electrode materials were measured by inductively coupled plasma-atomic emission spectrometry (ICP-AES) using an Atomscan Advantage (Thermo Jarrell Ash) spectrometer. An estimate of the levels of Zr and Al dopant was obtained by energy dispersive analysis of X-rays (EDAX) with a Noran Voyager II System. Powders were mixed with carbon, then spread onto a double-sided carbon conductive tape. The amount of water in the samples was determined with a Netzsch STA 409 thermal gravimetric analyzer.

Powder X-ray diffraction methods were used to determine phase purity. Diffraction data were collected on an automated Siemens D-5000 powder diffractometer with CuK<sub>α</sub> radiation. Unit-cell parameters were calculated by a least-squares refinement of the X-ray diffraction peak positions.

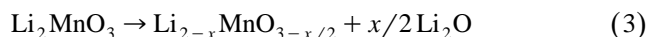
Electrodes consisted of the active oxide (80 wt.%), carbon (Vulcan XC-72, 10 wt.%), graphite (2 wt.%) and a polymer binder (polyvinylidene difluoride (Kynar), 8 wt.%). A slurry of the electrode mix in acetone (or tetrahydrofuran) was prepared and ball milled for several days.

Laminates were cast with a doctor blade from the slurry mix onto plate glass, from which the final electrodes were punched out. The electrodes were finally dried at 70–80°C (vacuum) overnight prior to cell assembly.

Galvanostatic discharge data were collected on 1225 or 2016 button cells containing a metallic lithium negative electrode, two Celgard 2400 separators, an electrolyte consisting of 1 M LiPF<sub>6</sub> in ethylene carbonate:dimethyl carbonate (50:50), and the positive electrode laminate. Cells were charged and discharged at constant current: 0.1 mA/cell for cell size 1225, and 0.3 mA/cell for cell size 2016.

### 3. Results and discussion

The structure of Li<sub>2</sub>MnO<sub>3</sub> is shown in Fig. 1. It consists of a cubic close-packed oxygen array in which layers of lithium ions are sandwiched between layers of manganese (67%) and lithium (33%) ions. Layered lithium-manganese-oxide compounds are produced by removing Li<sub>2</sub>O with acid according to the reaction:



The leaching process leaves the manganese ions in octahedral coordination in a layered arrangement and in a tetravalent state, but the oxygen array is left in an aBBaBBa.. stacking sequence to provide trigonal prismatic coordination for any remaining lithium in the original lithium-rich layer [18].

In terms of phase purity and crystallinity, the best leaching conditions for the Pechini-powders (pch-M/700C) and standard Li<sub>2</sub>MnO<sub>3</sub> samples (ss/500C) were carried out with 2.25–2.50 M H<sub>2</sub>SO<sub>4</sub> at room temperature for approximately 24 h. Transmission electron microscopy

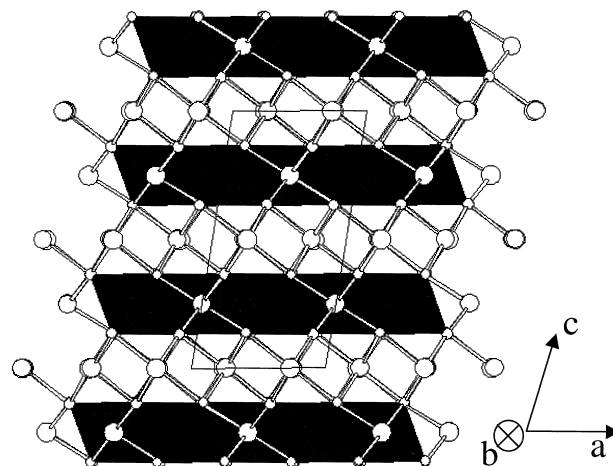


Fig. 1. The rock salt structure of Li<sub>2</sub>MnO<sub>3</sub> (standard material, C2/c,  $a = 4.932(6)$  Å,  $b = 8.537(9)$  Å,  $c = 9.600(10)$  Å,  $\beta = 99.15(5)^\circ$ , Volume = 404.2 Å<sup>3</sup>) [22]. The oxygen ions are unshaded small spheres, and the lithium ions are larger shaded spheres. Lithium and manganese ions are located in the center of the shaded octahedra.

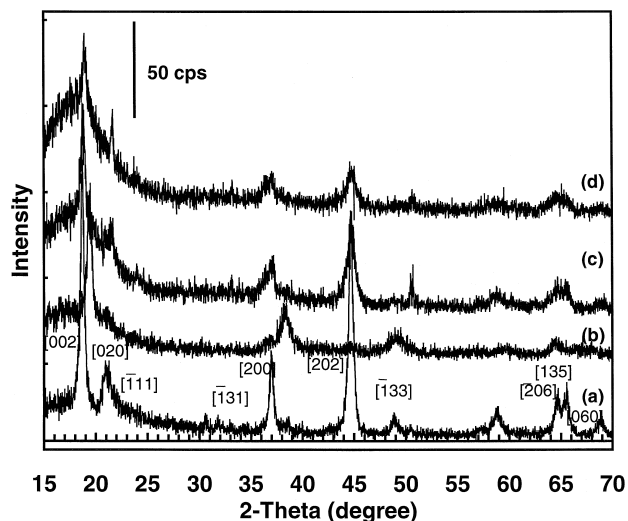


Fig. 2. X-ray powder diffraction patterns of (a) parent  $\text{Li}_2\text{Mn}_{0.95}\text{Zr}_{0.05}\text{O}_3$ ; (b)  $\text{Li}_{0.243}\text{Mn}_{0.935}\text{Zr}_{0.047}\text{O}_{2.122}$ ; acid-leached sample of (a); (c)  $\text{Li}_{0.854}\text{Mn}_{0.935}\text{Zr}_{0.047}\text{O}_{2.122}$  reaction of (b) with LiI; and (d)  $\text{Li}_{0.325}\text{Mn}_{0.935}\text{Zr}_{0.047}\text{O}_{2.122}$  reaction of (c) with  $\text{Br}_2$ .

data have shown that both pch-M/700C and ss/500C  $\text{Li}_{2-x}\text{MnO}_{3-x/2}$  products consist of large aggregates of small crystallites (50–100 nm) which have become porous, but still retain the same size, shape and bulk morphology of the parent materials [19]. Increasing the reaction time or acid concentration consistently produced an  $\alpha\text{-MnO}_2$  by-product. If the acid concentration was not sufficiently high, or if the surface area of the  $\text{Li}_2\text{MnO}_3$  phase was too low because of oversintered particles, then unreacted  $\text{Li}_2\text{MnO}_3$  remained in the product. These observations were consistent with those of Rossouw and Thackeray [15]. Therefore, the Pechini method was adopted to create materials with high surface area [16] and to provide an effective way to substitute manganese in the structure with other metal ions. In this respect, Zr can be fully substituted for manganese to yield the isostructural compound  $\text{Li}_2\text{ZrO}_3$  [20].

The initial acid-treatment step creates products that retain a significant portion of water. Even after drying at 40°C under vacuum, analysis by thermogravimetric methods showed that approximately 12 wt.% water remained in the products. The relatively small d-spacing of the lithium-deficient layers in the acid-treated compounds ( $d \sim 3.0$  Å) suggests that the resulting layered structures are unlike birnessite compounds, which contain water within the layers and give typical d-spacings of 7 or 11 Å. In

layered lithium manganese oxides derived from  $\text{Li}_2\text{MnO}_3$ , it appears that the water molecules (and protons) are located predominantly at the particle surface and are associated with grain boundaries. Nevertheless, the presence of protons within these layered structures cannot be discounted. Work is in progress to model and quantify the diffusivity of  $\text{H}^+$  ions in these materials by use of inelastic neutron scattering techniques.

Fig. 2 shows the X-ray diffraction patterns for (a) a Zr-substituted ( $\sim 5\%$ ) sample; (b) an acid-leached sample with an end composition of  $\text{Li}_{0.243}\text{Mn}_{0.935}\text{Zr}_{0.047}\text{O}_{2.122}$  in which some  $\text{Li}_2\text{O}$  has been removed; (c) a sample of (b) reacted with LiI to reintroduce lithium ions into the layered structure with a concomitant reduction of the manganese ions (i.e., not as  $\text{Li}_2\text{O}$ ); and (d) sample of (c) reacted with bromine to extract the lithium ions under non-aqueous conditions. Similar patterns were obtained for the unsubstituted compound and the Al-doped sample [21].

The extraction of  $\text{Li}_2\text{O}$  from the parent  $\text{Li}_2\text{Mn}_{0.95}\text{Zr}_{0.05}\text{O}_3$  (nominally 5 mol%) compound causes significant changes to the X-ray diffraction pattern (Fig. 2a and b); the changes arise predominantly because of the change in the stacking sequence of the oxygen ions [18]. Chemical lithiation of the  $\text{Li}_{0.243}\text{Mn}_{0.935}\text{Zr}_{0.047}\text{O}_{2.122}$  product with LiI at 80°C regenerates the close packed arrangement of the oxygen ions to yield a structure that closely resembles the layered  $\text{LiMnO}_2$  structure reported by Armstrong and Bruce [11] and Capitaine et al. [12] as shown by the X-ray diffraction pattern in Fig. 2c. It is of particular interest that re-oxidizing the lithiated product with bromine in chloroform does not significantly alter the X-ray diffraction pattern, indicating a retention of the layered structure. This result strongly suggests that the shearing of the cubic-close packed array of the parent  $\text{Li}_2\text{Mn}_{0.95}\text{Zr}_{0.05}\text{O}_3$  to form alternating layers of octahedra and trigonal prisms during the initial treatment with acid is associated with the removal (dissolution) of  $\text{Li}_2\text{O}$  from the structure. The unit cell parameters of these various materials, obtained by profile refinement of their X-ray diffraction patterns, are provided in Table 1.

Highly delithiated  $\text{Li}_{2-x}\text{MnO}_{3-x/2}$  products, where  $x > 1.9$ , transform on standing to a  $\gamma\text{-MnO}_2$  structure [21]. This process is accelerated if the oxide particle is in contact with carbon. This transformation was not observed with the zirconium-substituted samples, at least over a six month period, indicating their greater inherent stability to air.

Table 1  
Unit cell parameters of derivatives of  $\text{Li}_2\text{Mn}_{0.95}\text{Zr}_{0.05}\text{O}_3$  (C2/c)

Compound	Processing step	$a$ (Å)	$b$ (Å)	$c$ (Å)	$\beta$ (°)	Vol. (Å <sup>3</sup> )
$\text{Li}_2\text{Mn}_{0.95}\text{Zr}_{0.05}\text{O}_3$	Starting material	4.933(2)	8.511(4)	9.611(4)	100.09	397.3(3)
$\text{Li}_{0.243}\text{Mn}_{0.935}\text{Zr}_{0.047}\text{O}_{2.122}$	Acid-treatment	5.063(9)	8.589(20)	9.453(9)	98.98(17)	406.0(12)
$\text{Li}_{0.854}\text{Mn}_{0.935}\text{Zr}_{0.047}\text{O}_{2.122}$	LiI reduction	4.910(7)	8.604(14)	9.482(18)	99.4(2)	395.3(11)
$\text{Li}_{0.325}\text{Mn}_{0.935}\text{Zr}_{0.047}\text{O}_{2.13}$	$\text{Br}_2$ oxidation	4.934(9)	8.659(24)	9.516(12)	99.89(19)	400.5(14)

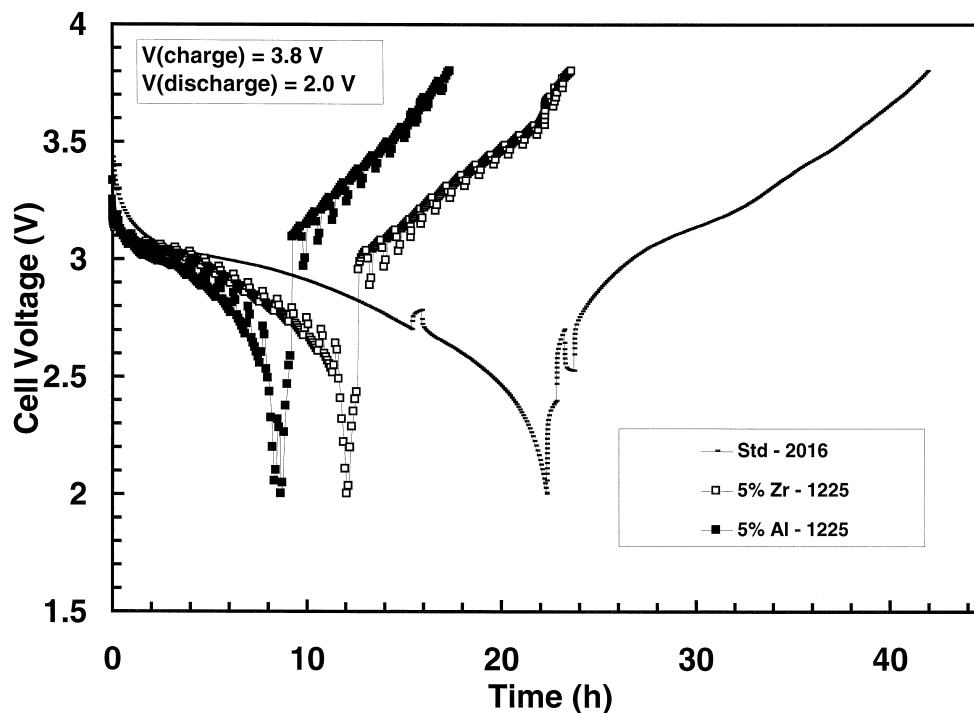


Fig. 3. First galvanostatic discharge/charge curves for cells with cathodes of standard  $\text{Li}_{0.106}\text{MnO}_{2.053}$  (2016 cell) (—),  $\text{Li}_{0.243}\text{Mn}_{0.935}\text{Zr}_{0.047}\text{O}_{2.122}$  (1225 cell) ( $\square$ ), and  $\text{Li}_{0.309}\text{Mn}_{0.95}\text{Al}_{0.05}\text{O}_{2.13}$  (1225 cell) ( $\blacksquare$ ). The breaks in the curves are open circuit tests to check the area specific impedance (ASI) of the cathode.

The initial discharge and charge profiles of lithium cells with  $\text{Li}_{0.106}\text{MnO}_{2.053}$  ( $\text{Li}_{2-x}\text{MnO}_{3-x/2}$ , where  $x = 1.894$ , from ss/500C  $\text{Li}_2\text{MnO}_3$ ), and Zr- and Al-substituted electrodes over a voltage range of 3.8 to 2.0 V are shown in Fig. 3. The relative stability to electrochemical cycling for

each of the cells is represented in Fig. 4 by plots of capacity vs. cycle number for the first ten cycles. The voltage profiles of the cells are similar. Although the discharge profiles indicate a single-phase reaction process, the charge process indicates that lithium is extracted in two

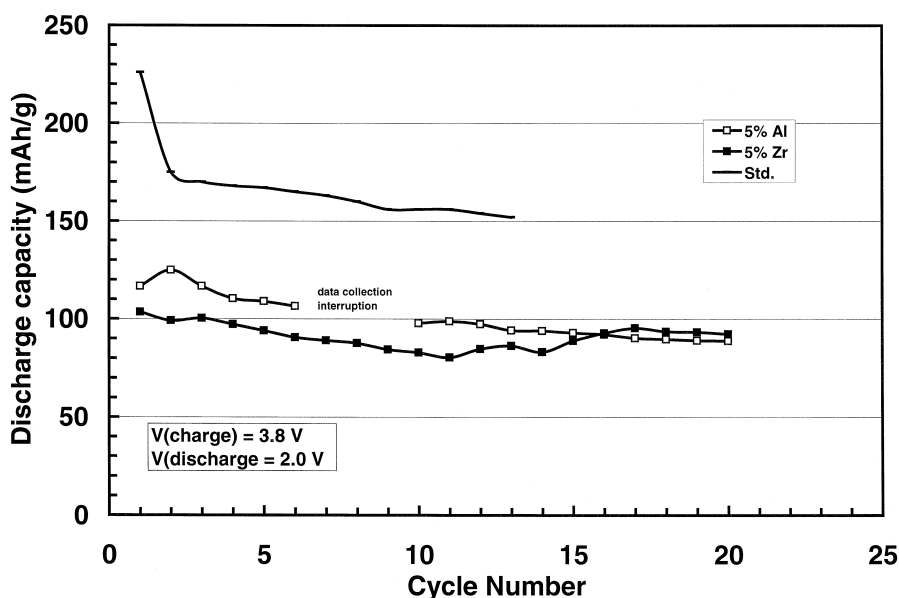


Fig. 4. Discharge capacity (mA h/g) vs. cycle number for three button cells consisting of standard  $\text{Li}_{0.106}\text{MnO}_{2.053}$  (2016 cell) (—),  $\text{Li}_{0.243}\text{Mn}_{0.935}\text{Zr}_{0.047}\text{O}_{2.122}$  (1225 cell) ( $\square$ ), and  $\text{Li}_{0.309}\text{Mn}_{0.95}\text{Al}_{0.05}\text{O}_{2.13}$  (1225 cell) ( $\blacksquare$ ).

stages, as is evident from the point of inflection approximately midway through charge. The two-stage process is consistent with earlier reports of  $\text{Li}_{2-x}\text{MnO}_{3-x/2}$  electrodes in lithium cells [15]. Somewhat surprisingly, the substituted electrode materials deliver an inferior capacity to the standard  $\text{Li}_{0.106}\text{MnO}_{2.053}$  electrode (Fig. 4), despite their apparent greater stability to air. They deliver an initial capacity between 100 and 120 mA h/g with a fade rate of about 1% mA h/g per cycle. By contrast, the standard  $\text{Li}_{0.106}\text{MnO}_{2.053}$  electrode delivered an initial capacity of 225 mA h/g and 157 mA h/g after 10 cycles with a fade rate of approximately 2% mA h/g per cycle after the initial discharge.

#### 4. Conclusions

An attempt has been made to stabilize layered lithium-manganese-oxide materials by acid treatment of the rock-salt phase  $\text{Li}_2\text{MnO}_3$ , in which some manganese has been substituted by zirconium and aluminum. Although the acid-treated Zr- and Al-substituted products are more stable to air, as manifest by a resistance to transforming to  $\gamma\text{-MnO}_2$ , their electrochemical properties are inferior to standard  $\text{Li}_{2-x}\text{MnO}_{3-x/2}$  ( $\text{Li}_{0.106}\text{MnO}_{2.053}$ ) electrodes.

#### Acknowledgements

Support for Argonne National Laboratory from the US Department of Energy's Advanced Battery Program, Chemical Sciences Division, Office of Basic Energy Sciences, under Contract No. W31-109-Eng-38 is also grate-

fully acknowledged. Dr. Lisa M. Utschig (ANL) is thanked for her technical assistance in acquiring ICP-AES data.

#### References

- [1] T. Ohzuku, H. Fukuda, T. Hirai, *Chemistry Express* 2 (1987) 543.
- [2] P. Strobel, *Proc. Mater. Res. Soc. Symp.* 293 (1993) 63.
- [3] P. Strobel, C. Mouget, *Mater. Res. Bull.* 28 (1993) 93.
- [4] P. Strobel, J.C. Charenton, *Rev. de Chim. Miner.* 23 (1987) 125.
- [5] P. Strobel, J.C. Charenton, M. Lenglet, *Rev. de Chim. Miner.* 24 (1987) 199.
- [6] M. Tsuji, S. Komarneni, Y. Tamaura, M. Abe, *Mater. Res. Bull.* 27 (1992) 741.
- [7] F. Leroux, D. Guyomard, Y. Piffard, *Solid State Ionics* 80 (1995) 299.
- [8] F. Leroux, D. Guyomard, Y. Piffard, *Solid State Ionics* 80 (1995) 307.
- [9] S. Bach, J.P. Periera-Ramos, N. Baffier, *J. Electrochem. Soc.* 143 (1996) 3429.
- [10] R. Chen, P. Zavalij, M.S. Whittingham, *Chem. Mater.* 8 (1996) 1275.
- [11] A.R. Armstrong, P.G. Bruce, *Nature* 381 (1996) 499.
- [12] F. Capitaine, P. Gravereau, C. Delmas, *Solid State Ionics* 89 (1996) 197.
- [13] G. Vitins, K. West, *J. Electrochem. Soc.* 144 (1997) 2587.
- [14] Y. Shao-Horn, S.A. Hackney, A.R. Armstrong, P.G. Bruce, R. Gitzendanner, C.S. Johnson, M.M. Thackeray, *J. Electrochem. Soc.* (1999) in press.
- [15] M.H. Rossouw, M.M. Thackeray, *Mater. Res. Bull.* 26 (1991) 463.
- [16] M.P. Pechini, US Patent 3,330,697, 1967.
- [17] J.M. Tarascon, D. Guyomard, *J. Electrochem. Soc.* 138 (1991) 2864.
- [18] M.H. Rossouw, D.C. Liles, M.M. Thackeray, *J. Solid State Chem.* 104 (1993) 464.
- [19] T.E. Bofinger, S.A. Hackney, unpublished data.
- [20] National Bureau of Standards, (US) Monograph 25 1957 (1982)
- [21] C.S. Johnson, data to be published.
- [22] M. Jansen, R. Hoppe, *Z. Anorg. Allg. Chem.* 397 (1973) 279.